

All-optical pulse data generation in a semiconductor optical amplifier gain controlled by a reshaped optical clock injection

Gong-Ru Lin, Yung-Cheng Chang, and Kun-Chieh Yu

Citation: [Applied Physics Letters](#) **88**, 191114 (2006); doi: 10.1063/1.2203213

View online: <http://dx.doi.org/10.1063/1.2203213>

View Table of Contents: <http://scitation.aip.org/content/aip/journal/apl/88/19?ver=pdfcov>

Published by the [AIP Publishing](#)

Articles you may be interested in

[Ultrafast all-optical switching via coherent modulation of metamaterial absorption](#)

Appl. Phys. Lett. **104**, 141102 (2014); 10.1063/1.4870635

[40 GHz small-signal cross-gain modulation in 1.3 \$\mu\text{m}\$ quantum dot semiconductor optical amplifiers](#)

Appl. Phys. Lett. **93**, 051110 (2008); 10.1063/1.2969060

[Femtosecond switching with semiconductor-optical-amplifier-based Symmetric Mach–Zehnder-type all-optical switch](#)

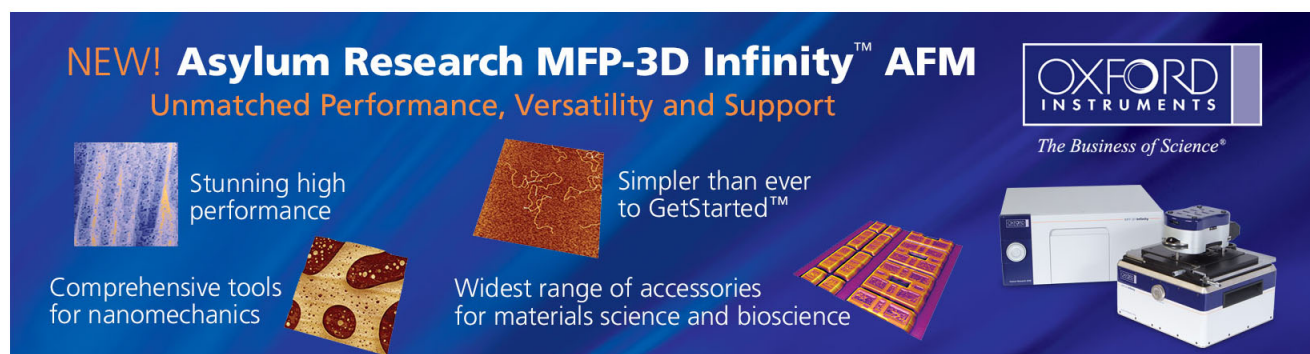
Appl. Phys. Lett. **78**, 3929 (2001); 10.1063/1.1379790

[Observation of dark-pulse formation in gain-clamped semiconductor optical amplifiers by cross-gain modulation](#)

Appl. Phys. Lett. **75**, 3760 (1999); 10.1063/1.125447

[The wavelength-dependent transfer function for optically controlled semiconductor lasers](#)

J. Appl. Phys. **83**, 5056 (1998); 10.1063/1.367322



NEW! Asylum Research MFP-3D Infinity™ AFM
Unmatched Performance, Versatility and Support

OXFORD INSTRUMENTS
The Business of Science®

Stunning high performance
Simpler than ever to GetStarted™
Comprehensive tools for nanomechanics
Widest range of accessories for materials science and bioscience

The advertisement features several images: a textured surface, a circular pattern, a grid of small components, and the MFP-3D Infinity AFM instrument itself.

All-optical pulse data generation in a semiconductor optical amplifier gain controlled by a reshaped optical clock injection

Gong-Ru Lin,^{a)} Yung-Cheng Chang, and Kun-Chieh Yu

Department of Photonics and Institute of Electro-Optical Engineering, National Chiao Tung University, 1001 Ta Hsueh Road, Hsinchu, Taiwan 300, Republic of China

(Received 26 October 2005; accepted 28 March 2006; published online 10 May 2006)

Wavelength-maintained all-optical pulse data pattern transformation based on a modified cross-gain-modulation architecture in a strongly gain-depleted semiconductor optical amplifier (SOA) is investigated. Under a backward dark-optical-comb injection with 70% duty-cycle reshaping from the received data clock at 10 GHz, the incoming optical data stream is transformed into a pulse data stream with duty cycle, rms timing jitter, and conversion gain of 15%, 4 ps, and 3 dB, respectively. The high-pass filtering effect of the gain-saturated SOA greatly improves the extinction ratio of data stream by 8 dB and reduces its bit error rate to 10^{-12} at -18 dBm. © 2006 American Institute of Physics. [DOI: 10.1063/1.2203213]

All-optical data processing has been comprehensively investigated owing to the implementation of versatile optical logic gates and data format conversion. Previously, numerous laser diode or semiconductor optical amplifier (SOA) based ultrafast all-optical data pattern transforming architectures^{1–9} have emerged via the effects of the direct or the cross gain modulation,^{2,3} interferometer related cross-phase modulation (XPM),^{4,5} SOA-based wavelength conversion,⁶ SOA-based nonlinear optical loop mirror (NOLM),⁷ Fabry-Perot laser diode based dual-wavelength injection locking,⁸ and under threshold scheme,⁹ etc. Typically, a wavelength- or format-converted data pattern can be demonstrated at a bit rate of >10 Gbits/s due to the subnanosecond carrier lifetime of the optically cross-gain-modulated (XGM) SOA, in which the gain recovery process is strongly affected by the injection-power dependent nonlinearity.¹⁰ Since the wavelength conversion mechanism relies strictly on the significant gain saturation of the SOA caused by the intense injection, a relatively high power of the input data pattern at original wavelength is thus mandatory. Such an operation is somewhat impractical in a real network with interfacial data pattern transforming requirement since the level control (usually the level amplification) of the optical data stream is required. Recently, a modified XGM technique has emerged to precisely control the gain of the SOA in the time domain by injecting a dark-optical-comb reshaped optical clock,¹¹ which simultaneously enhances the XGM depth and the modulation bandwidth of the SOA. Obviously, the SOA can be controlled by a reshaped optical clock to offer extremely high XGM depth and narrow gain window, which should be an alternative to achieve the high bit-rate pulse data pattern transformation. In this letter, we propose for the first time a high-power dark-optical-comb pulse injection architecture to temporally control the gain of the SOA, providing a sufficient XGM depth for a pulse data pattern transformation at low input levels. With the injection of such a reshaped optical clock, the parametric analyses on wave form, extinction ratio, and sensitivity of the SOA transformed pulse data pattern are reported. The gain-shifting and high-pass filtering mechanisms of the SOA corresponding to

the enhanced bit-error-rate and signal-to-noise ratio performances are elucidated.

Figure 1(a) schematically depicts the SOA-based pulse data pattern transformer. In experiment, an optical non-return-to-zero (NRZ) formatted pseudorandom binary sequence (PRBS) signal with pattern length of $2^{31}-1$ is employed as the input data stream. A radio-frequency synthesizer (Agilent, E8457A) at 10 GHz simulates the electrical clock for the data generator and the pulse data pattern transformer. The output power of the optical NRZ PRBS data stream is attenuated to -1 dBm with its wavelength coincident with the peak wavelength of the SOA gain spectrum. The pulse data pattern transformer is configured by the traveling-wave typed multi-quantum-well SOA (QPhotonics LLC, QSOA-1550) and a backward optical injecting source. The small signal gain and typical output power of the single-mode-fiber pigtailed and butterfly packaged SOA are 20 dB and 15 mW, respectively. As shown in Fig. 1(b), the ampli-

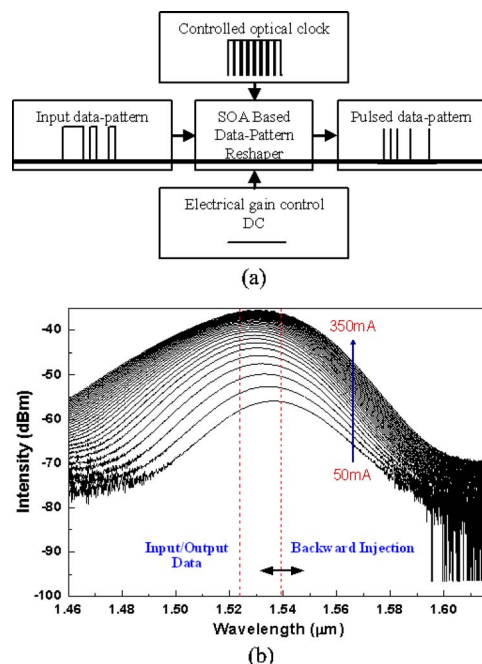


FIG. 1. (a) The schematic diagram of a SOA-based data pattern transformer; (b) ASE spectra of SOA at different biasing currents and the operating principle of a dark-optical-comb pulse-train generator.

^{a)} Author to whom correspondence should be addressed; electronic mail: grlin@faculty.nctu.edu.tw

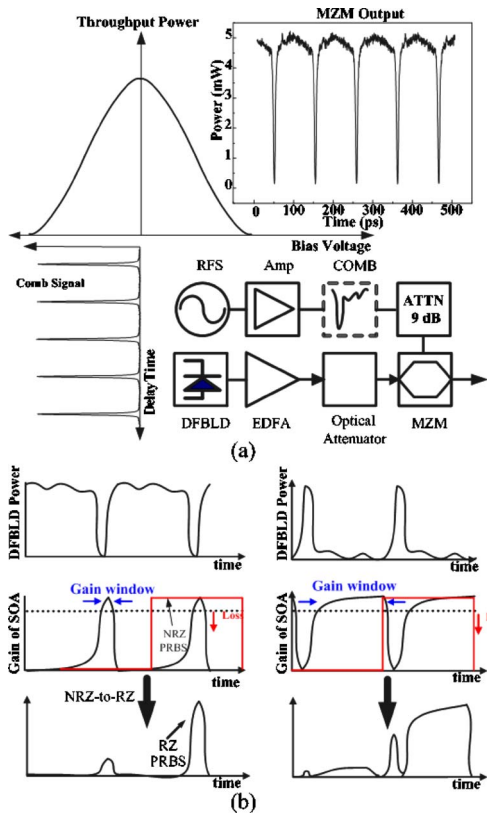


FIG. 2. (a) The operating principle of a dark-optical-comb pulse-train generator; (b) the illustration of the data pattern transformation processes in a SOA under the backward dark (left) and bright (right) optical-comb injection conditions.

fied spontaneous emission (ASE) of the SOA ranges between 1510 and 1550 nm, which exhibits a 3-dB spectral linewidth of 35 nm and a peak wavelength of 1530 nm under a biased current of 280 mA. The key components of the backward optical injector are a tunable laser, a 10-GHz electrical comb generator, and a Mach-Zehnder intensity modulator (MZM).¹¹ The dark-optical-comb pulse train is obtained by passing the tunable laser output through the MZM operated at nonlinear region (without dc bias), as shown in Fig. 2(a). The electrical comb generator triggered by the amplified electrical clock (with power of 26.4 dBm) from the aforementioned radio-frequency synthesizer is used to drive the MZM for generating dark-optical-comb pulse train. To gain deplete the SOA at highly biased condition, the dark optical comb is then amplified to 18 dBm by using an erbium-doped fiber amplifier (EDFA) and backward injected into the SOA via an optical circulator. To perform the bit-error-rate (BER) analysis at 10 Gbits/s, the transformed data pattern is detected by a high-gain avalanche photodiode (APD) incorporating a gain-controlled amplifier and a clock/data recovery circuit. The pulse data pattern is analyzed by a digitized sampling oscilloscope (Agilent, 86100+86109A) and a bit-error-rate detector (Agilent, 71612C).

In principle, an input data pattern is transformed into a pulsed one in the SOA when the backward injected optical clock turns off, as illustrated in Fig. 2(b). The effect of the backward injected wave form on the gain window and the transformed pattern shape in SOA can be simulated by solving the modified rate equations of time-varied carrier density (N_j), input data (P_i), and backward injected (P_b) signals with

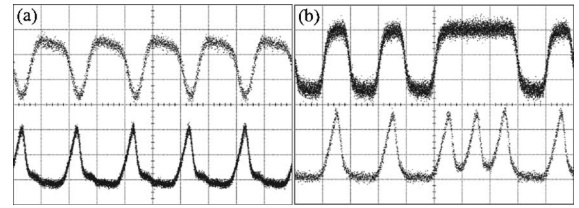


FIG. 3. (a) Upper: the dark optical comb injected into SOA; lower: the generated pulse train under a cw input. (b) Upper: the input data stream with 10101110 pattern; lower: the pulse data stream transformed by SOA.

average powers of $\bar{P}_{m,j}$ and $\bar{P}_{s,j}$ in j th gain section of the SOA, as listed below:

$$\frac{\partial N_j(z, T)}{\partial T} = \frac{I}{qV} - \frac{N_j}{\tau_C} \left\{ \frac{\Gamma g_{m,j}[N_j(z, T)]}{\hbar \omega_m A_{\text{cross}}} \bar{P}_{m,j} + \frac{\Gamma g_{s,j}[N_j(z, T)]}{\hbar \omega_s A_{\text{cross}}} \bar{P}_{s,j} \right\}, \quad (1)$$

$$\frac{\partial P_{m,j}(z, T)}{\partial z} = -\Gamma \{g_{m,j}[N_j(z, T)] - \alpha_{\text{int}}\} P_{m,j}(z, T), \quad (2)$$

$$\frac{\partial P_{s,j}(z, T)}{\partial z} = \Gamma \{g_{s,j}[N_j(z, T)] - \alpha_{\text{int}}\} P_{s,j}(z, T), \quad (3)$$

where I , A_{cross} , and V denote the injection current, cross-section area in active area, and volume of the SOA; q is the electron charge; $\hbar \omega_i$ and $\hbar \omega_b$ denote the input and backward injected photon energies; τ_C denotes the spontaneous emission lifetime; and α_{int} , g_i , and g_b are the internal loss and asymmetric gain coefficients in the SOA. Our simulation reveals that the pulse width as well as the duty cycle of the data pattern can be narrowed down as the duty cycle and the peak amplitude of the backward injected wave form greatly increase. Shrinking the gain window of the SOA in the time domain is mandatory to optimize the pulse data pattern transformation. By contrast, the backward optical injection of the typical pulse train with short pulse width only causes a broader and reshaped gain window with insufficient gain-depletion depth in the SOA, which consequently generates a nontransformed but seriously distorted data pattern,¹¹ as illustrated in Fig. 2(b). The wave forms of the backward injected dark-optical-comb pulse train and the output of the SOA under a cw input are shown in Fig. 3(a). Under an electrical comb pulse width of 40 ps at 10 GHz, the duty cycle of the dark optical comb generated from the MZM is up to 80%. The pulsation of the input data pattern results from a serious gain depletion and a greatly narrowed gain window in the SOA backward injected by large duty-cycle signal. For example, a NRZ data stream (10101110) encounters the residual gain in the SOA and transforms into a pulse pattern, as shown in Fig. 3(b).

On the other hand, the use of the high-level electrical pumping accompanied by a strong optical injection to concurrently suppress lasing and enhance carrier/photon interaction in the SOA can significantly result in a transforming speed larger than the carrier recovery rate of the SOA.¹⁰ The speed limitation for the SOA-based data pattern transformer is determined by the gain recovery time of the SOA. The gain recovery time τ in the SOA is described as $\tau^{-1} = \tau_{\text{nr}}^{-1} + aS$,¹⁰ where τ_{nr} is the nonradiative recombination time, a is the stimulated emission rate, and S is the internal photonden-

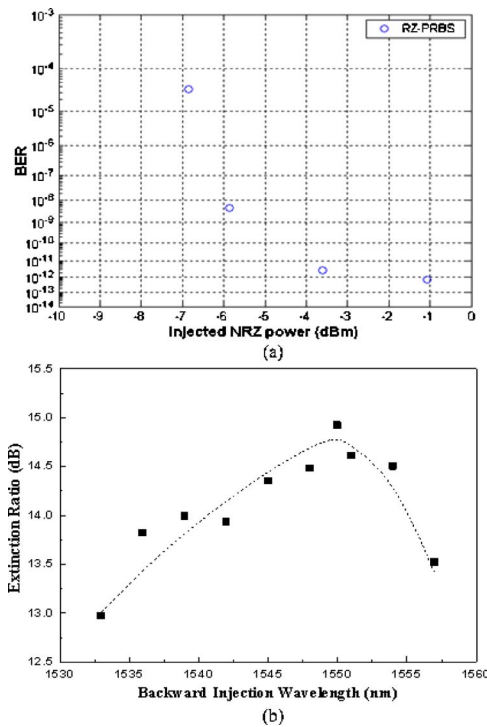


FIG. 4. (a) The bit error rate measured at different input data powers; (b) the extinction ratio of the transformed pulse data stream as a function of backward injecting wavelength.

sity in the SOA. It is elucidated that the gain recovery time of the SOA as well as the rising time of the transformed pulse data pattern can be effectively shortened by greatly increasing the internal photon density of the SOA after strong backward injection. The backward injection of the dark optical comb with extremely large duty cycle thus results in an ultranarrow gain window with enhanced switching response, facilitating the convertible data rate up to 10 Gbits/s and beyond. A nearly error-free ($\text{BER} < 10^{-12}$) pulse data stream can be achieved at a received optical power of -19 dBm. Such an excellent performance is correlated with the less fluctuated signal amplitude and the improved signal-to-noise ratio of the transformed pulse data stream, which originates from the gain-saturation induced high-pass filtering effect in the SOA operated at high-gain condition.¹³ In principle, such a self-gain modulation effect in SOA can further be enhanced by increasing the input power. As expected, the BER of the pulse data pattern significantly decreases from 10^{-8} to 10^{-12} as the input data power increases from -6 to -1 dBm, as shown in Fig. 4(a).

Furthermore, such an operation further enhances the extinction ratio (defined as the power ratio of the data level “1” to the data level “0”) of the transformed data pattern under a backward injection at longer wavelength. This result is mainly attributed to both the XGM induced by strong injection power and the large red shift in the gain spectrum of the SOA at the data wavelength. The effect of the injected dark-optical-comb wavelength on the extinction ratio of the RZ PRBS is determined and is shown in Fig. 4(b). We observed that the extinction ratio of the input data at 1530 nm is greatly improved from 7 to 14.9 dB after the pulse data pattern transformation in the SOA with a backward injection at 1550 nm. In fact, the trend of the extinction ratio almost coincides with that of the SOA gain spectrum. The shift in gain spectrum of the SOA is given by $\lambda_N = \lambda_0 - \kappa_0(N - N_0)$,¹² where κ_0 is a constant and λ_N and λ_0 denote the peak wave-

lengths of the SOA gain spectrum at carrier densities of N (under backward injection) and N_0 (transparency), respectively. It is seen that a blueshift of the SOA gain spectrum occurs when operating the SOA at a high-gain ($N \gg N_0$) condition. Meanwhile, the intense optical injection strongly depletes the carriers as well as gain of the SOA within most of one period. This changes the SOA from gain to loss condition ($N < N_0$) and also leads to a redshift in the gain spectrum of SOA. It is thus desirable to locate the data wavelength at the gain peak of the unsaturated SOA, as the gain depletion at this wavelength is more pronounced than others. Such a high-gain and strong-injection induced gain-shift effect further benefits from the advantage of raising extinction ratio in the SOA transformed pulse data pattern. In this case, the gain shape of SOA not only depletes but also shifts to longer wavelength by means of backward dark-optical-comb injection. Experimentally, the enhancement on extinction ratio of the transformed pulse data pattern strictly relies on the backward injecting wavelength. Under constant backward injecting power, a shorter data wavelength could result in a deeper gain depletion as well as better extinction ratio at the output. In other words, the power required to deplete the gain of SOA strongly depends on the data wavelength.¹⁴

In conclusion, a modified cross-gain-modulation architecture is demonstrated by using a backward dark-optical-comb injected SOA for all-optical pulse data pattern transformation of the low-power input data stream at an identical wavelength. The transformed pulse data stream exhibits a duty cycle, a rms timing jitter, and a conversion gain of 15%, 4.2 ps, and 3 dB, respectively. The signal-to-noise ratio and the extinction ratio of the input data stream can be greatly improved owing to the high-pass filtering effect of the SOA operating at a saturated gain condition. The input power dependent carrier lifetime shortening effect of the SOA further benefits from the increasing on transforming bit rate up to 10 Gbits/s with a nearly error-free performance.

This work is supported in part by the National Science Council, Taiwan R. O. C. under Grant No. NSC94-2215-E009-040.

¹C. G. Lee, Y. J. Kim, C. S. Park, H. J. Lee, and C.-S. Park, *J. Lightwave Technol.* **23**, 834 (2005).

²D. Norte and A. E. Willner, *IEEE Photonics Technol. Lett.* **8**, 712 (1996).

³D. Norte and A. E. Willner, *IEEE Photonics Technol. Lett.* **8**, 715 (1996).

⁴B. Mikkelsen, M. Vaa, H. N. Poulsen, S. L. Danielsen, C. Joergensen, A. Kloch, P. B. Hansen, K. E. Stubkjaer, K. Wunstel, K. Daub, E. Lach, G. Laube, W. Idler, M. Schilling, and S. Bouchoule, *Electron. Lett.* **33**, 133 (1997).

⁵L. Xu, V. Baby, I. Glesk, and P. R. Prucnal, *IEEE Photonics Technol. Lett.* **15**, 308 (2003).

⁶P. S. Cho, D. Mahgerefteh, and J. Goldhar, *Proceedings of the 24th European Conference on Optical Communication, Madrid, Spain, 20–24 September* (IEEE, New York, 1998), Vol. 1, p. 353.

⁷H. J. Lee, S. J. B. Yoo, and C.-S. Park, *Proceedings of the Optical Fiber Communication Conference and Exhibit, Anaheim, CA, 17–22 March 2001* (IEEE, New York, 2001), Vol. 1, p. MB7-1.

⁸C. W. Chow, C. S. Wong, and H. K. Tsang, *Opt. Commun.* **209**, 329 (2002).

⁹Y. C. Chang, Y. Lin, J. H. Chen, and G.-R. Lin, *Opt. Express* **12**, 4449 (2004).

¹⁰J. M. Wiesenfeld, B. Glance, J. S. Perino, and A. H. Gnauck, *IEEE Photonics Technol. Lett.* **5**, 1300 (1993).

¹¹G.-R. Lin, I. Chiu, and M. Wu, *Opt. Express* **13**, 1008 (2005).

¹²I. D. Henning, M. J. Adams, and J. V. Collins, *IEEE J. Quantum Electron.* **2**, 609 (1985).

¹³K. Sato and H. Toba, *IEEE J. Sel. Top. Quantum Electron.* **7**, 328 (2001).

¹⁴K. Inoue, T. Mukai, and T. Saitoh, *Electron. Lett.* **23**, 328 (1987).